

Short Communication

Synthesis of Au@PtAuAg Yolk–Shell Nanoalloy as an Electrocatalyst for Methanol Oxidation Reaction

Zirong Li^{1,*}, Jiajing Li², Zhenghua Wang^{2,*}

¹ College of Chemistry and Materials Engineering, Anhui Science and Technology University, Bengbu, Anhui, China, 233000

² College of Chemistry and Materials, Anhui Normal University, Wuhu, Anhui, China, 241000

*E-mail: lizir@ahstu.edu.cn

Received: 1 January 2019 / Accepted: 9 February 2019 / Published: 10 March 2019

Au@PtAuAg yolk–shell nanoalloy composed of an Au nanoparticle core and a PtAuAg shell was synthesized via a simple wet-chemical method. The Au@PtAuAg nanoalloy was applied as an electrocatalyst for methanol oxidation reaction, and it shows a good electrocatalytic activity and better anti CO poison ability than that of commercial Pt/C catalysts. The better electrocatalytic performance of the Au@PtAuAg yolk–shell nanoalloy was possibly due to the electronic effect by Au and Ag that could facilitate the elimination of the intermediate during methanol oxidation.

Keywords: yolk–shell nanoalloy; Au@PtAuAg; methanol oxidation

1. INTRODUCTION

Direct methanol fuel cells (DMFC) are regarded as the most promising power source in the future and can be applied to mobile devices and portable devices. [1-3] Concerning the catalysts for DMFC, Pt based materials are widely used. However, there are still drawbacks for Pt catalysts, such as low efficiency, high cost, poor stability and durability. These drawbacks limit the employment of DMFC to a large extent [1-10]. Thus, increase the activity and stability of Pt catalysts as well as reducing the cost of Pt catalysts will be more practical for the development of DMFC.

The activity of the catalysts is related to their size, composition and morphology. It is worth mention that the core-shell nanoparticles have attracted great attention because of their unique structure. For example, Yang et al. synthesized hollow or caged noble metal nanoparticles, which shown good methanol oxidation activities in DMFC anode. [11] Geng et al. found that Au-Pt nucleus-shell nanostructured catalyst showed an excellent activity for DMFC, and had a significant CO-poisoning

resistance.[12] Qiao et al. reported that the catalysts composed of Pd nanoparticles and PMO core-shell structures had a higher conversion rates and selectivity in the alcohol oxidation reaction .[13] In addition, core-shell structured material can be used in many other fields, especially in heterogeneous catalysis. The core-shell structure is a special extension of the nuclear-shell structure, which is composed of a solid particle as the core, a certain gap between the core and the shell, and the porous shell in most cases. Nuclear/interstitial/shell structural materials are of interest not only because of their unique structure, but also because of their many important roles .[14-20] For example, sintered stable materials can be based on such systems. The encased metal nanoparticles are successfully encased in a casing to prevent migration and further sintering with other metal nanoparticles. In addition to the anti-sintering stability, the core/shell structure materials also have a good monodisperse and narrow particle size distribution. This makes these materials very suitable as model catalysts and allows the study of general problems in heterogeneous catalysis, such as particle size dependence of catalyst activity or metal-carrier interaction.

In this study, Au@PtAuAg yolk-shell nanoalloy was synthesized by a convenient wet-chemical method. Trisodium citrate was applied as a reducing agent to obtain Au nanoparticles in the first step. Then, ascorbic acid was added to reduce Au, Ag and Pt simultaneously, and the Au@PtAuAg yolk-shell nanoalloy was finally obtained. The electrocatalytic performances of the Au@PtAuAg yolk-shell nanoalloy toward methanol oxidation reaction were investigated by electrochemical tests. The results showed that the electrocatalytic performance and stability of the Au@PtAuAg yolk-shell nanoalloy was higher than that of commercial Pt/C catalysts.

2. EXPERIMENTAL

2.1. Chemicals

Pt/C catalyst was purchased from Johnson Matthey Corp. Ascorbic acid, chloroplatinic acid, silver nitrate, methanol, chloroauric acid, sulfuric acid, trisodium citrate, absolute ethyl, alcohol and Nafion were purchased from Sinopharm Chemical Reagent Co., Ltd. (Shanghai, China). All the chemical reagents were of analytical grade and used as received without further purification. Deionized water was used throughout the experiment.

2.2 Synthesis methods

The Au@PtAuAg yolk-shell nanoalloy was synthesized by a two-step method. In the first step, 2 mL 0.002 M HAuCl₄, 1 mL 0.1 M C₆H₅Na₃O₇·2H₂O and 5 mL deionized water were added in a beaker. Then, the beaker was heated in a water bath at 60 °C for 20 min under constant shaking at a frequency of 60 round per minute (RPM). In the second step, 2 mL 0.002 M H₂PtCl₆, 4 mL 0.002 M AgNO₃ and 1 mL 0.1 M ascorbic acid were added into the above solution. The beaker was further heated in the water bath at 60 °C for 40 min under constant shaking at 60 RPM. The final product was collected by centrifugation and washed with deionized water and absolute ethanol in turn.

2.3 preparation of working electrode

A glassy carbon electrode (GCE) with a diameter of 3 mm (active surface area of 0.071 cm²) was polished by slurry of alumina powder, and then cleaned by deionized water. A certain amount of catalyst was evenly dispersed in 1000 μ L deionized water by ultrasonication. After that, 8 μ L of the catalyst suspension was dropped onto the GCE. After the catalyst suspension was dried, 6 μ L of 0.5% Nafion was dropped onto the GCE. The GCE was dried in air before use. The mass loading of Pt on GCE is about 8 μ g for all the catalysts.

2.4 Characterizations

The morphology, structure and composition of the samples were characterized by scanning electron microscopy (SEM), transmission electron microscopy (TEM), energy scattering spectrum, X-ray powder diffraction (XRD) and X-ray photoelectron energy spectrum (EDS). Among them, SEM adopts S-4800 scanning electron microscope from Hitachi Company with an acceleration voltage of 5 kV. TEM and HRTEM were obtained by FEI Tecnai G2 20 high resolution electron microscopy with an acceleration voltage of 200 kV. The composition and purity of all products were analyzed by Bruker D8 Advance XRD. X-ray source using $\lambda = 0.15406$ nm Cu Ka radiation, 40 kV X-ray tube voltage and current 40 mA, scanning step length of about 0.028°. EDS is analyzed by HORIBA EMAX energy spectrometer attached to the above SEM.

2.5 Electrochemical tests

The electrochemical performances were tested by using a three-electrode cell on a CHI-660D model electrochemical workstation (CHI Ins. Shanghai, China) at room temperature. The reference electrode was a saturated calomel electrode (SCE), and the auxiliary electrode was a platinum electrode (2cm \times 2cm).

In the cyclic voltammetry (CV) tests, the scanning rate was 50 mV s⁻¹, and the potential window was -0.2 ~ 1.0 V. The electrolytes were N₂ saturated 0.5 M H₂SO₄ solution or N₂ saturated 0.5 M H₂SO₄ + 0.5 M CH₃OH solution. The data were recorded after the figure tend stable. The chronoamperometry experiments were performed at 0.6 V for 3600 s in 0.5 M H₂SO₄ + 0.5M CH₃OH.

3. RESULTS AND DISCUSSION

The crystallographic structure of the Au@PtAuAg yolk-shell nanoalloy was investigated by XRD. As displayed in Fig. 1a, three broad diffraction peaks at 38.57°, 44.77° and 65.26° were observed. These diffraction peaks can be indexed to the (111), (200) and (220) crystal planes of face-centered cubic phase crystal. By comparing the standard pattern of Au (JCPDS card no. 4-784), Ag (JCPDS card no. 4-783) and Pt (JCPDS card no. 4-802), the diffraction peaks are not coincide with any of the pure Au, Ag and Pt. This result reveals that an alloy of Pt–Au–Ag was formed. Furthermore, EDS spectrum was

recorded to identify the chemical constituents of the sample, as displayed in Fig. 1b. The presence of Pt, Au and Ag elements confirmed the elemental composition of the sample. The Pt/Au/Ag atomic ratio was 1 : 1 : 2.43, which is very close to the initial feeding ratio.

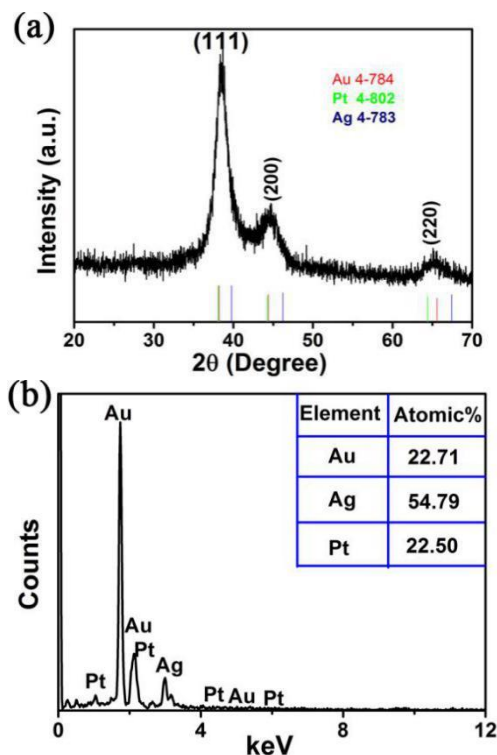


Figure 1. (a) XRD pattern of the nanoalloy sample; (b) EDS spectrum of the sample.

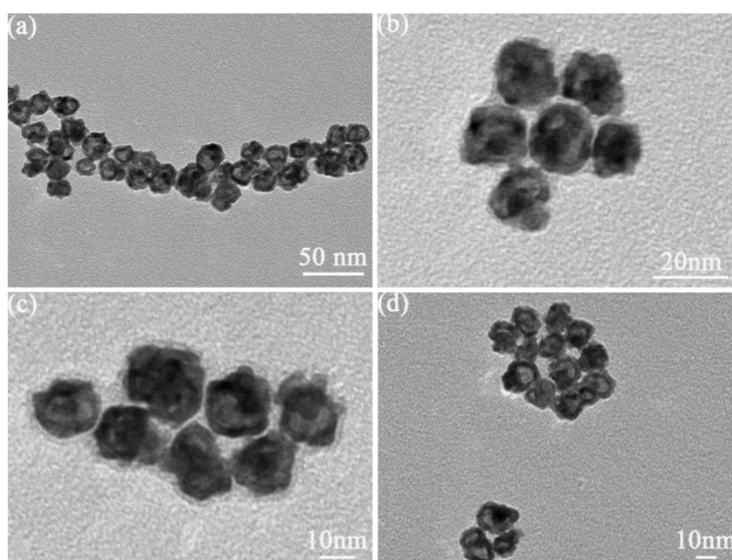


Figure 2. TEM images of rich Au core-PtAuAg yolk-shell structure.

The morphology of the alloy composite was further elucidated by TEM. Fig.2a-d depicts the characteristic TEM images of the Au@PtAuAg yolk-shell nanoalloy with different magnification. It can be clearly seen that the sample contained a yolk and eggshell structure composite nanoparticles with a diameter of about 15 nm, indicating that the product is mainly composed of the core shell nanoparticles.

The detailed structure and element distribution of Au@PtAuAg yolk-shell nanoalloy were characterized by HRTEM. HRTEM image was shown in Fig. 3a and the calculated lattice fringe spacing was 0.202 nm, which is less than the lattice spacing of (200) crystal surface of Au (0.203 nm) and (200) crystal surface of Ag (0.204 nm), but larger than that of Pt (200) crystal surface (0.196 nm). STEM was performed to analyse Au@PtAuAg yolk-shell nanoalloy as shown in Fig.3b. Clearly, the results confirmed the structure of the alloys was Au rich core and PtAgAu shell. Thus, the lattice fringe spacing strongly suggested the formation of alloys among three metals.

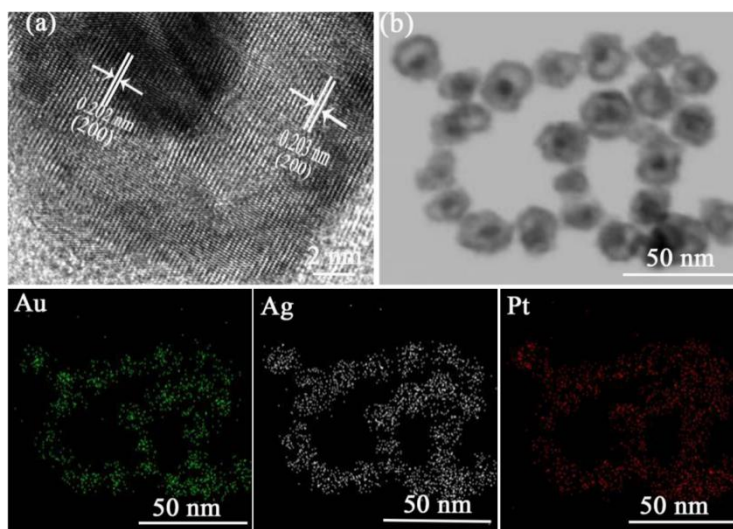


Figure 3. (a) HRTEM image, (b) STEM image and elemental mappings of the rich Au core-PtAuAg yolk-shell structure.

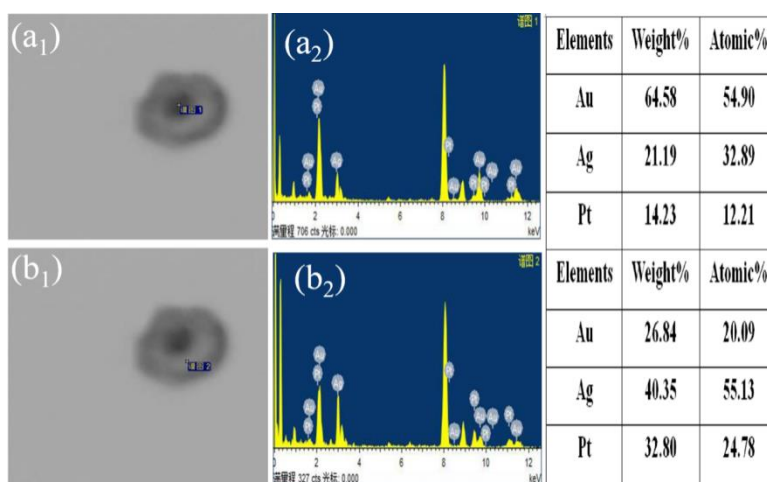


Figure 4. STEM-EDS point analysis of the rich Au core-PtAuAg yolk-shell structure: (a) from the center of the particle, and (b) from the edge.

Furthermore, in order to confirm the structure, a particle was selected and EDS analysis was performed at different placed. As shown by the results, the core of the alloy was composed by ~ 54.90 atomic% of Au, 32.89 atomic % of Ag and 12.21 atomic% of Pt. However, the shell was composed by

20.09 atomic% of Au, 55.13 atomic % of Ag and 24.78 atomic% of Pt. In our previous work, it was found that under 338 K, the CA could not efficiently reduce the AuCl_4^- and led to the formation of some Au atom clusters. [21]

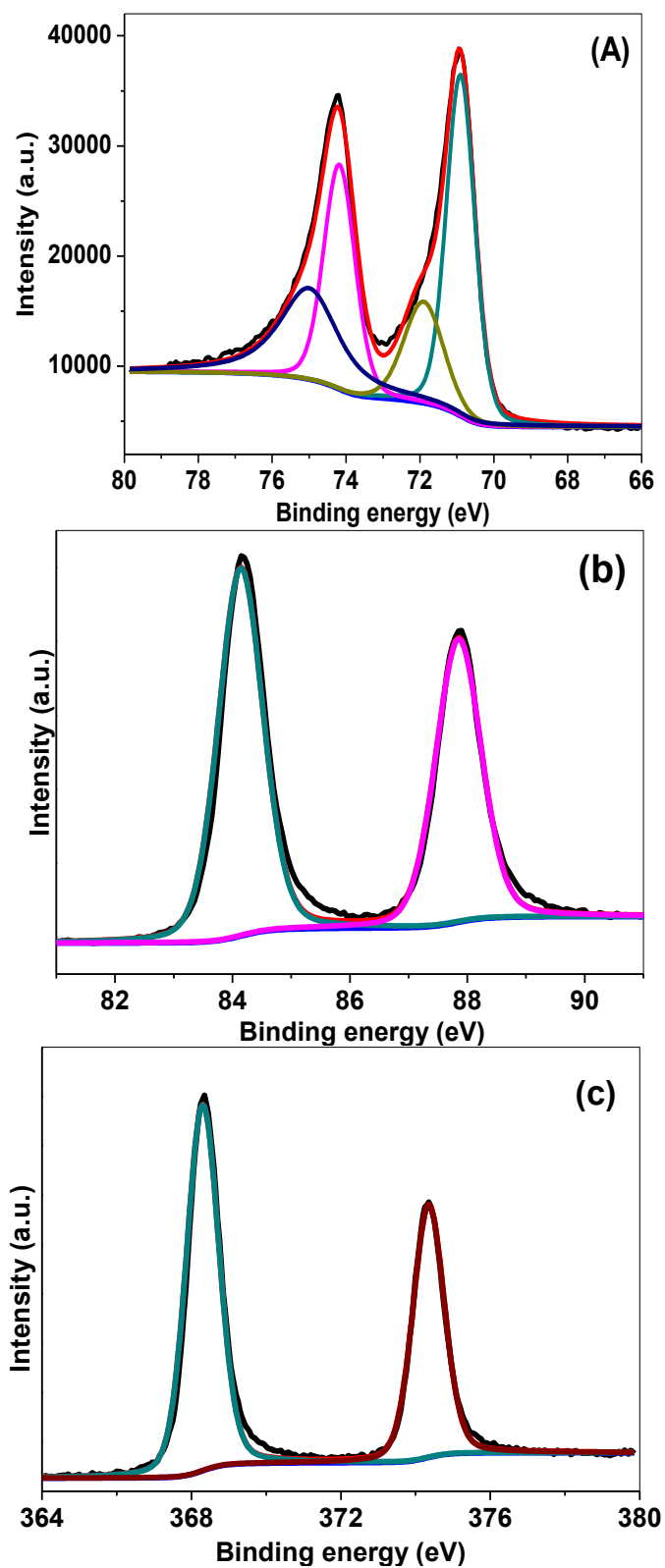


Figure 5. XPS spectrum of Pt 4f (A), Au 4f (B) and Ag 3d (C).

After AgNO_3 and PtCl_6^- were added into the solution, on the one hand, due to the reducing ability of AA, Ag ions could be reduced first around the Au core and also serve as the reducing agent for the transformation of a small part of PtCl_6^- to Pt (0), which possibly resulted in the formation of core shell structure via Kirkendall effect. On the other hand, the possibility of the reducing AgCl around the Au core would also contribute to the formation of core shell structure. Then, due to the relatively stronger reducing ability of AA and as well as the CA and Ag atoms surrounded the Au core formed as above, the rest of PtCl_6^- , some AuCl_4^- and Ag^+ or AgCl could be totally reduced by AA, which led to the formation of PtAuAg shell. In addition, a controlled experiment of the synthesis of PtAu nanostructure without AgNO_3 was performed and the results suggested that the yolk-shell structure cannot be obtained.

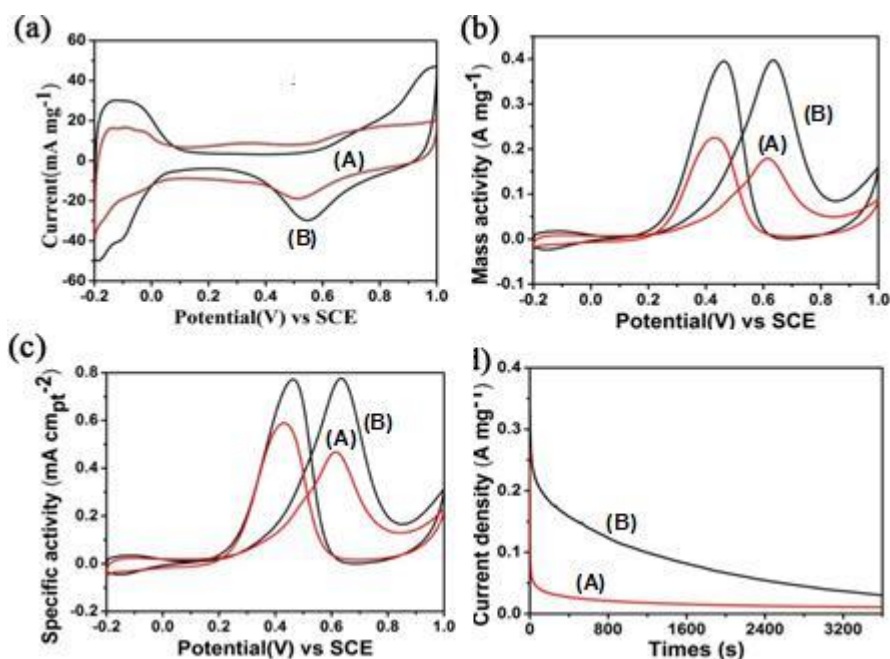


Figure 6. (a) CV curves of the catalysts in 0.5 mol L⁻¹ N₂-saturated H₂SO₄ solution; (b, c) CV curves of the catalysts in 0.5 mol L⁻¹ H₂SO₄ and 0.5 mol L⁻¹ CH₃OH solution; (d) Chronoamperograms of different catalysts for MOR at 0.60 V for 3600 s of Pt/C (A) and the Au @PtAuAg yolk-shell structure (B).

Furthermore, the chemical state of the Au@PtAuAg yolk-shell nanoalloy was studied by XPS and the results were displayed in Fig.5. Clearly, the main peaks at 71.0 and 74.2 eV were ascribed to the signal of the metallic Pt 4f and in addition, another two peaks were also observed as indicated by the peaks at 75.5 and 72.6 eV, which is similar to the fact that indicating the presence of PtO/Pt(OH)₂ in the previous work.[22-25] Besides, the metallic Au and Ag was noticed as shown by Fig.5b and c, which indicated by the peaks at 84.2 and 87.7 eV for Au 4f as well as 368.4 and 374.3 eV for Ag 3d. Thus, the present synthesis successfully resulted in the formation of trimetallic alloys.

In order to investigate the electrocatalytic activity of Au@PtAuAg yolk-shell nanoalloy, cyclic voltammetry (CV) and chronoamperometry of different catalysts were measured. Fig. 6a shown the CV curve of different catalysts in N₂ saturated 0.5 M H₂SO₄. The electrochemical effective area (ECSA) of the catalyst can be calculated by integral deduction of the area of hydrogen adsorption and desorption between the -0.2 and 0.1 V. The ECSA of Au@PtAuAg yolk-shell nanoalloy and commercial Pt/C

catalyst were 51.14 and $38.26 \text{ m}^2 \cdot \text{g}^{-1}$, respectively. Compared with the calculated results, the ECSA of Pt-Au-Ag sample was larger than that of commercial Pt/C catalyst.

As shown the results in Figure 6b, a higher peak current was obtained by Au@PtAuAg yolk-shell nanoalloy ($390 \text{ mA} \cdot \text{mg}^{-1} \text{ Pt}$) than that of commercial Pt/C ($194 \text{ mA} / \text{mg Pt}$) at $\sim 0.62 \text{ V}$. As compared in Figure 6c, the Au@PtAuAg yolk-shell nanoalloy had a higher activity in term of specific area. Finally, Chronoamperometry is employed to study the electrochemical activity and stability of the catalyst. As can be seen from Figure 6d, the nanoalloy had a much better stability compared with the Pt/C. After 3200 s, the current density of the nanoalloy is higher ($50 \text{ mA} \cdot \text{mg}^{-1} \text{ Pt}$) by factor of 5 times than Pt/C ($11.0 \text{ mA} \cdot \text{mg}^{-1} \text{ Pt}$), further demonstrating the better electrocatalytic durability.

Finally, the mass activity of Pt based nanomaterials with Ag, Au and Ru was compared to demonstrate the advantage of the present catalyst. As shown in Table 1, the yolk-shell structure of our catalyst was more active than some PtAu, PtAg and PtRu bimetallic catalyst, indicating a promising application for methanol oxidation.

Table 1. Comparison of Pt-based nanomaterials for methanol electrooxidation

Catalysts	I_f (mA/mg Pt)	Refs.
Au@PtAuAg	390	This work
Pt ₃ Ru/Ru	348	24
Pt _{0.05} ^Au/C	163	26
Au@Pt _{0.57} Ag _{0.43} NRs	~ 38	26
Pt-Au alloy	348	27
Au-Pt nanowire	340	28
Au@Pt	149	29
PtAg (core-shell)	271	30

4. CONCLUSIONS

In conclusion, Au@PtAuAg yolk-shell nanoalloy was synthesized successfully by a simple method. The obtained nanoalloy was well characterized by a series of methods and used as catalyst for the electrooxidation of methanol. It was found that the alloy had a better performance and stability for the methanol oxidation compared to commercial Pt/C catalyst, which demonstrated the advantages of the core-shell structure with unique core/void/shell structure and different components.

ACKNOWLEDGEMENT

The Key Project of Anhui Science and Technology University (ZRC2016477), as well as the Open Project (KF201601) of Key lab of Novel Thin Film Solar Cells are greatly appreciated for the financial support. Zirong Li also wants to thank the Key Research and Development Projects(1804a09020075) of Anhui Province and the project (AKZDXK2015AO1) in AHSTU for the financial support.

References

1. Ermete. Antolini, *J. Power Sources*, 170(1)(2007)1.
2. E. Antolini, E. R. Gonzalez, *Appl. Catal. B-Environ.*, 63 (2006,)137
3. U. B. Demirci, *J. Power Sources*, 173(11)(2007) 11.
4. N. Kakati, J. Maiti, S. H. Lee, S. H. Jee, B. Viswanathan, Y. S. Yoon, *Chem. Rev.*, 114 (1)(2014) 12397.
5. H. S. Liu, C. J. Song, L. Zhang, J. J. Zhang, H. J. Wang, D. P. Wilkinson, *J. Power Sources*, 155(2)(2006)95.
6. N. S. Porter, H. Wu, Z. W. Quan, J. Y. Fang, *Acc. Chem. Res.*, 46(2013)1867.
7. Y. K. Zhou, K. Neyerlin, T. S. Olson, S. Pylypenko, J. Bult, H. N. Dinh, T. Gennett, Z. P. Shao, *Energ. Environ. Sci.*, 10 (2010)1437.
8. X. Q. Huang, S. H. Tang, X. L. Mu, Y. Dai, G. X. Chen, Z. Y. Zhou, F. X. Ruan, Z. L. Yang, N. F. Zheng, *Nat. Nanotechnol.*, 6 (2011) 28.
9. S. J. Guo, E. K. Wang, *Acc. Chem. Res.*, 44(2011)491.
10. S. Sakong, A. Gross, *Acs Catal.*, 6(2016) 5575.
11. H. Liu, J. Qu, Y. Chen, J. Li, F. Ye, J. Y. Lee, J. Yang, *J. Am. Chem. Soc.*, 134(2012)11602.
12. L. Kuai, S. Wang, B. Geng, *Chem. Commun.*, 47(2011) 6093.
13. J. Liu, H. Q. Yang, F. Kleitz, Z. G. Chen, T. Yang, E. Strounina, *Adv. Funct. Mater.*, 22(2012)591.
14. P. M. Arnal , M. Comotti , F. Schüth , *Angew. Chem. Int. Ed.*, 45(2006) 8224.
15. S. H. Joo , J. Y. Park , C. K. Tsung , Y. Yamada , P. Yang , G. A. Somorjai, *Nat. Mater.*, 8(2009)126 .
16. M. Feyen, C. Weidenthaler, R. Güttel, K. Schlichte, U. Holle, A. H. Lu, F. Schüth, *Chem. Eur. J.*, 17(2011)598.
17. M. Feyen, C. Weidenthaler, F. Schüth, A. H. Lu, *Chem. Mater.*, 22(2010) 2955.
18. A. H. Lu, W. C. Li, N. Matoussevitch, B. Spliethoff, H. Bönnemann, F. Schüth, *Chem. Commun.*, 98(2005) 268.
19. J. C. Park, J. U. Bang, J. Lee, C. H. Ko, H. Song, *J. Mater. Chem.*, 20(2010) 1239.
20. L. M. Liz-Marzán, M. Giersig, P. Mulvaney, *Langmuir.*, 12(1996) 4329.
21. J. J. Li, H. Rong, X. W. Tong, P. Wang, T. Chen, Z. H. Wang, *J. Colloid Interface Sci.*, 513(2018) 251.
22. Y. H. Zhang, J. J. Li, H. Rong, X. W. Tong, Z. H. Wang, *Langmuir*, 33(2017)5991.
23. L. Bai, *Appl. Sur. Sci.*, 433 (2018) 279.
24. L. Bai, Y. W. Bai, *J. Nanopart. Res.*, (2018) 20: 24. <https://doi.org/10.1007/s11051-018-4135-4>.
25. J. N. Zheng, S. S. Li, X. H. M, F. Y. Chen, A. J. Wang, J. R. Chen, J. J. Feng, *J. Mater. Chem. A*, 2 (2014) 8386.
26. L. L. Feng, G. Gao, P. Huang, X. S. Wang, C. L. Zhang, J. L. Zhang, S. W. Guo, D. X. Cui, *Nanoscale Res. Lett.*, 6 (2011) 551.
27. J. T. Zhang, H. Y. Ma, D. J. Zhang, P. P. Liu, F. Tian, Y. Ding, *Phys. Chem. Chem. Phys.*, 10 (2008) 3250.
28. W. Hong, J. Wang, E. K. Wang, *Small*, 10 (2014) 3262.

29. Z. G. Guo, X. Zhang, H. Sun, X. P. Dai, Y. Yang, X. S. Li, T. T. Meng, *Electrochim Acta*, 134 (2014) 411.
30. M. P. Mercer, D. Plana, D.J. Fermín, D. Morgan, N. Vasiljevic, *Langmuir*, 31 (2015) 10904.

© 2019 The Authors. Published by ESG (www.electrochemsci.org). This article is an open access article distributed under the terms and conditions of the Creative Commons Attribution license (<http://creativecommons.org/licenses/by/4.0/>).